DOI: https://doi.org/10.3897/arphapreprints.e72208

Status emendation of *Mustela aistoodonnivalis* (Mustelidae: Carnivora) based on molecular phylogenetic and morphology

Yingxun Liu, Yingting Pu, Xuming Wang, Xin Wang, Rui Liao, Keyi Tang, Chen Shunde, Bisong Yue, Liu Shaoying

Yingxun Liu
Sichuan Academy of Forestry.
18# Xinghui Xilu road, Chengdu 61008, Sichuan, PR China.
Tel: 86-13684035370
kunrei@163.com

Running title: The taxonomic status of *Mustela aistoodnnivalis*

Status emendation of *Mustela aistoodonnivalis* (Mustelidae: Carnivora) based on molecular phylogenetic and morphology

Yingxun Liu [#], Yingting Pu [#], Xunming Wang, Xin Wang , Rui Liao , Keyi Tang , Shunde Chen *, Bisong Yue * , Shaoying Liu *
[1]Sihcuan Academy of Forestry, Chengdu 610066, Sichuan, PR China. No.18, Xinghui Xilu Road, Chengdu 610081, Sichuan, China. (YL, XW, XW, RL SL)
[2]College of Life Science, Sichuan Normal University, Chengdu 610101, Sichuan, PR China. (YP, KT,SC)
[3]College of Life Sciences, Sichuan University, Chengdu 610065, Sichuan, PR China. (YL, BY)
*Corresponding author

Abstract: The missing-toothed pygmy weasel, *Mustela aistoodonnivalis* Wu and Kao, 1991, was originally described from Zhouzhi and Zhashui in the Qingling Mountains in Shaanxi province, China. Subsequently it was considered a subspecies of *M. nivalis.* During a faunal survey of northwest Sichuan, some specimens of *M. aistoodonnivalis* were collected. Molecular phylogenetic studies showed that *M. aistoodonnivalis* formed a distinct clade that was sister to *M. eriminea* based on one mitochondrial gene and six nuclear genes. Morphologically, there was an obvious difference between *M. aistoodonnivalis* and *M. nivalis,* especially the lack of the second lower molar. Geometric morphology studies and species delimitation analysis revealed the valid species status of *M. aistoodonnivalis*. In summary, we confirm that *M. aistoodonnivalis* is an independent species rather than a subspecies of *M. nivalis*, and that it is more closely related to *Mustela eriminea*.

Key words*:* geometric morphology*, Mustela aistoodonnivalis, Mustela nivalis,* second lower molar phylogeny, species identification.

Introduction.

Mustela aistoodonnivalis was described by Wu and Kao (1991) as a new species in Mustelidae. Wu and Kao (1991) collected four specimens of *M. aistoodonnivalis* from Zhouzhi and Zhashui County of Shaanxi province, and described the external morphology and skull of *M. aistoodonnivalis*: the body was similar to *M. nivalis* and it had a longer tail, which was longer than 1/3 of the head and body length; the dorsal pelage was dark brown in summer; due to the missing second lower molar (M_2), the total number of teeth was 32. The taxonomic position of this species of *Mustela* has been controversial: following Hutterer (2005), Smith and Xie (2009) and Lin and Motokawa (2010) followed *M. aistoodonnivalis* as a subspecies of *M.*

nivalis and considered the lack of M_2 a variable characteristic seen in other *M. nivalis* populations. At the same time, several Chinese scholars, such as Ruan and Gong (1999), Wang (2003), Qin *et al.* (2004), Hu and Hu (2007), Pan *et al.* (2007), Gong *et al.* (2009) and Jiang *et al*.（2005, 2007）have rejected the taxonomic authority of Hutterer (2005) and considered *M. aistoodonnivalis* an independent species.

According to Mittermeier and Wilson (2009), the genus *Mustela* contains 17 species, seven of which are distributed in China. Generally, the usual size of *Mustela* species is 20-40 cm, and the largest *Mustela* species is 56 cm, while *M. nivalis* is a smaller species of weasel. *M. nivalis* was originally described form Sweden (Linnaeus 1766) and is defined by the color of tail tip, the smaller skull size and baculum morphology (Sheffield and King 1994). In China, *M. nivalis* is distributed in Xinjiang, Heilongjiang, Jilin, Liaoning, Inner Mongolia, Shanxi, western Sichuan, and Taiwan. It contains several named subspecies, *M. nivalis aistoodonnivalis* Wu and Cao,1991, *M. nivalis nivalis* Linnaeus, 1766, *M. nivalis stoliczkana* Blanford,1877, *M. nivalis russelliana* Thomas,1911, *M. nivalis tonkinensis* Björkegren,1941 and one unnamed subspecies form Taiwan (Smith and Xie 2009; Lin and Motokawa 2010), but Mittermeier and Wilson (2009) classified all subspecies in China as one subspecies. Among them, Wu and Kao (1991) considered the *M. russelliana* distributed in Sichuan a close relative to *M. aistoodonnivalis.*

Following Wu and Kao (1991), we found 6 specimens that fit the described morphological characteristics of *M. aistoodonnivalis*, and we further used molecular phylogeny, and geometric morphology to determine whether this species is valid.

Methods.

Ethics statement.

All samples were obtained following the regulations of China for the implementation of the protection of terrestrial wild animals (State Council Decree [1992] No. 13). Collecting was approved by the Ethics Committee of Sichuan Academy of Forestry (no specific permit number). Voucher specimens were deposited in Sichuan Academy of Forestry, Chengdu, China.

Sampling and sequencing. —— A total of 24 Mustelinae specimens from 10 localities in China were collected, including 4 individuals of *M. altaica*, 10 individuals of *M. sibirica*, 6 individuals of *M. aistoodonnivalis*, 2 individuals of *M. nivalis*, and 2 individuals of *Neovison vison* (Table 1，Fig.1). All collected specimens were identified based on external characteristics according to Smith and Xie (2009) and Pan *et al.* (2007). Voucher specimens were deposited in the Sichuan Academy of Forestry. We also collected muscle and liver tissue in 95% ethanol and these were subsequently stored at -75 °C for molecular studies.

Table 1 Samples and sequences of *Mustela* used for molecular analyses

Genus	Species	Species ID	Locality	Genbank accession No.						
				APOB	ATP7A	BDNF	CYTB	RAG1	RAG2	TMEM20
Mustela	*aistoodonnivalis*	csd2000	Jiuzhai, Sichuan	MT888695	MT888710	MT888725	MT888740	MT888758	MT888773	MT888788
Mustela	*aistoodonnivalis*	csd2001	Jiajinshan, Sichuan	MT888696	MT888711	MT888726	MT888741	MT888759	MT888774	MT888789
Mustela	*aistoodonnivalis*	csd2015	Li County, Sichuan	MT888706	MT888721	MT888736	MT888751	MT888769	MT888784	MT888799
Mustela	*aistoodonnivalis*	csd2339	Wanglang, Sichuan	MT888707	MT888722	MT888737	MT888752	MT888770	MT888785	MT888800
Mustela	*altaica*	csd2003	Pulan, Tibet	MT888698	MT888713	MT888728	MT888743	MT888761	MT888776	MT888791
Mustela	*altaica*	csd891	Ruoergai, Sichuan	MT888708	MT888723	MT888738	MT888754	MT888771	MT888786	MT888801
Mustela	*altaica*	csd2002	Xilinhot, Nei Mongol	MT888697	MT888712	MT888727	MT888742	MT888760	MT888775	MT888790
Mustela	*erminea*	csd2004	Heishui, Sichuan	MT888699	MT888714	MT888729	MT888744	MT888762	MT888777	MT888792
Mustela	*nivalis*	csd1480	Fushun, Liaoning	MT888694	MT888709	MT888724	MT888739	MT888757	MT888772	MT888787
Mustela	*nivalis*	csd2011	Hejing, Xinjiang	MT888705	MT888720	MT888735	MT888750	MT888768	MT888783	MT888798
Mustela	*sibirica*	csd2005	Hanyuan, Sichuan	MT888700	MT888715	MT888730	MT888745	MT888763	MT888778	MT888793
Mustela	*sibirica*	csd2006	Hanyuan, Sichuan	MT888701	MT888716	MT888731	MT888746	MT888764	MT888779	MT888794
Mustela	*sibirica*	csd2007	Hanyuan, Sichuan	MT888702	MT888717	MT888732	MT888747	MT888765	MT888780	MT888795
Mustela	*sibirica*	csd2008	Hanyuan, Sichuan	MT888703	MT888718	MT888733	MT888748	MT888766	MT888781	MT888796
Mustela	*sibirica*	csd2009	Hanyuan, Sichuan	MT888704	MT888719	MT888734	MT888749	MT888767	MT888782	MT888797
Mustela	*sibirica*	csd2379	Hanyuan, Sichuan				MT888753			
Neovison	*vison*	csd2349	Emin, Xinjiang				MT888755			
Neovison	*vison*	csd2352	Emin, Xinjiang				MT888756			

All the gene fragments were amplified with published primers. PCR amplifications were performed in a reaction volume mixture of 25 µl, containing 12.5 µl 2×Taq Master Mix (Vazyme, Nanjing, China), 1 µl each primer, 1 µl genomic DNA and 9.5 µl double distilled water. PCR conditions for *cyt b* amplifications consisted of an initial denaturing step at 94°C with 5 min followed by 38 cycles of denaturation at 94°C with 45s, annealing at 49°C with 45s, extension at 72°C with 90s, and then a final extension step at 72°C with 12 min. PCR conditions for those nuclear genes were basically the same as that of the *cyt b* sequences, but we changed the annealing temperature to 49-56°C degrees. PCR products were checked on a 1.0% agarose gel and purified subsequently using ethanol precipitation. Purified PCR products were directly sequenced using the BIG DYE TERMINATOR CYCLE KIT V3.1 (Applied Biosystems, Foster City, CA, USA) and determined with an ABI 310 ANALYZER (Applied Biosystems).

In order to test the phylogenetic relationship within Chinese *Mustela* species and to evaluate the species status of *M. aistoodonnivalis*, we downloaded *cyt b* sequences and *Rag1*, *Rag2*, *ATP7A*, *BDNF*, *TMEM20*, and *Apob* sequences of *Mustela* species from GenBank for comparison (Table 2).

Table 2 Genbank accession numbers of download sequence from NCBI

Species	CYTB	RAG2	ATP7A	BDNF	TMEM20	APOB	RAG1
Mustela altaica	AB026100						
	KC815122						
	AB051239						
Mustela erminea	AF057127	EF987991	EF987575	EF987619	EF988033	EF987522	AB109347
	AB026101						
	KM091450						
	EF088939						
Mustela eversmanni	EF987741	EF987992	EF987576	EF987620	EF988034	EF987523	EF987973
	KT224449						
Mustela nivalis	EF987744	EF987995	EF987580	EF987624	EF988037	EF987526	EF987976
	HM106319						
	AB046612						
	AB564129						
Mustela sibirica	EF987747	EF987998	EF987583	EF987627	EF988039	EF987529	EF987979
Mustela strigidorsa	EF987748	EF987999	EF987584	EF987628		EF987530	EF987980
	AB119078						
	AB305635						
Mustela kathiah	HM106320						
	AB285331						
	JQ965760						
Mustela frenata	AF498153	EF472425	EF987577	EF987621	EF472442	EF472296	EF472412
	HM106321						
	GQ153578						
Mustela lutreola	EF987742	EF987993	EF987578	EF987622	EF988035	EF987524	EF987974
	AB026105						
Mustela nigripes	EF987743	EF987994	EF987579	EF987623	EF988036	EF987525	EF987975
	GQ153574						

	GQ153575						
Mustela nudipes	EF987745	EF987996	EF987581	EF987625		EF987527	EF987977
	AB285332						
Mustela putorius	EF987746	EF987997	EF987582	EF987626	EF988038	EF987528	EF987978
	HM106318						
	KT693383						
Mustela africana	GQ153570						
Mustela felipei	GQ153571						
Mustela itatsi	AB026104		LC124879	LC124912		AB285338	AB285384
Neovison vison	AF057129	DQ660281	EF987585	DQ660205	EF472443	DQ660191	DQ660268
	KM488625						
Lutra lutra	AF057124	EF472419	EF987568	EF987611	EF472436	EF472290	EF472406
	FJ236015						
Lutra sumatrana	EF472347	EF472422	EF987571	EF987614	EF472439	EF472293	EF472409
	KY117556						

Phylogenetic analysis.

DNA sequences were aligned and examined, and heterozygote screening of nuclear gene fragments was carried out in MEGA 5 (Tamura *et al*. 2011). All *cyt b* sequences obtained were checked carefully and queried in BLAST searches of GenBank to assess the homology of the species we obtained.

Phylogenetic analyses were conducted on the following three datasets: 1) complete mitochondrial *cyt b* genes; 2) combined all six nuclear genes fragments; 3) combined all genes. We applied Bayesian inference (BI) to evaluate phylogenetic relationships within Chinese *Mustela* species with three datasets. BEAST V1.7.5 was used for BI analyses (Drummond *et al*. 2012). *Lutra lutra* and *Lutra sumatrana* were used as outgroups in our analysis. The best model of evolution for each gene was determined using Akaike information criterion (AIC) in the JMODELTEST V2 (Table 3). BEAST analyses used a random starting tree, a birth-death tree prior, an uncorrelated exponentially relaxed molecular clock and the program's default prior distributions of model parameters. Each analysis ran 100 million generations and sampled every 5,000th generation. The runs were combined using the Log combiner module of BEAST with a burn-in of 10%. Posterior probabilities (PP) > 0.95 between two branches were considered to be strongly supported (Huelsenbeck and Rannala 2004).

Species tree and Species delimitation.

According to the results of the phylogenetic analysis for datasets 1, we first calculated the *p*-distances for dataset 1 between all species with

1,000 bootstrap replicates to summarize sequence divergences based on *cyt b* in MEGA 5 (Nei M. and Kumar S. 2000; Tamura *et al.* 2011). Next, based on a coalescent-based method, the species tree was restructured for datasets 3 and implemented in *BEAST (Heled and Drummond 2010). Based on the results of the phylogenetic analysis for datasets 1, we assigned the samples into 13 putative species (including 2 outgroup species). The best-fit models were calculated using jModeltest and were provided in Table 3. The same priors as phylogenetic analyses described above were used in the species tree calculation. Each analysis was run for 100 million generations and sampled every 5,000th generation (Heled and Drummond 2010). The computational results were combined using the Log combiner module of BEAST with a burn-in of 10%.

Table 3 Gene symbol, primer sequences and the best model of evolution for each gene segments used in the study.

Gene symbol	Primers	The best model
Cytb[a]	L14724: CGAAGCTTGATATGAAAAACCATCGTTG	GTR+I+G
	H15915: GGAATTCATCTCTCCGGTTTACAAGAC	
APOB[b]	F: GTGCCAGGTTCAATCAGTATAAGT	GTR+I+G
	R: CCAGCAAAATTTTCTTTTACTTCAA	
ATP7A[c]	F: TCCCTGGACAATCAAGAAGC	HKY+G
	R: AAGGTAGCATCAAATCCCATGT	
BDNF[c]	F: CATCCTTTTCCTTACTATGGTT	K80
	R: TTCCAGTGCCTTTTGTCTATG	
RAG1[d]	F: GCTTTGATGGACATGGAAGAAGACAT	SYM+I+G
	R: GAGCCATCCCTCTCAATAATTTCAGG	
RAG2[c]	F: TCATGGAGGGAAAACACCAAA	K80+I+G
	R: TGCACTGGAGACAGAGATTC	
TMEM20[e]	F: TGGGTTTATAGGCCCCAAAG	HKY
	R: CACGTKGGCACATYRTTA	

[a] primer from (Irwin *et al*., 1991); [b] primer from (Heather *et al*., 2003); [c] primer from (Murphy *et al*., 2001); [d] primer from (Teeling *et al.*, 2000); [e] primer from (Lindblad-Toh K *et al.*, 2005)

SPLITS V 1.0.19 (Species Limits by Threshold Statistics) of the R statistical environment was used for species delimitation analyses of dataset 1 with outgroups removed (Fujisawa and Barraclough 2013). Generalized mixed Yule-coalescent model (GMYC) was used for defining the transitions between interspecific and intraspecific diversification processes to delimit the genetic cluster SPLITS as putative species (Pons *et al.* 2006). These analyses were implemented in the R PACKAGE APE (Paradis *et al.* 2004), which used the time-calibrated gene tree of *cyt b* as the input tree. The number of putative species was identified using a single threshold.

Multilocus coalescent delimitation was implemented in BPP V 2.1 based on dataset 3 (Ziheng and Bruce 2010). According to the results of the restructured species tree, after excluded outgroup species, we assigned these samples to 11 putative species. This species tree was also used as guide trees in multilocus coalescent delimitation. Two reversible jump Markov chain Monte Carlo (rjMCMC) algorithms (algorithms 0 and 1) were used for species delimitation. Based on the suggestion of software manual, when using algorithm 0, finetune (e) was used 2, 10 or 20; when using algorithm 1, finetune (a, m) were used (1, 0.5), (1.5, 1) or (2, 2) (Yang and Rannala 2010). Gamma-distributed priors G (6, 6,000) was used on the population size parameters (θs), and the age of the root in the species tree (τ0) was assigned Gamma-distributed priors G (4, 1,000). The analyses for each data set were repeated 12 times, and each jMCMC was run for 100,000 generations and sampled every 5 generations after discarding 50,000 generations as burn-in (Yang and Rannala 2010).

Geometric morphometric analyses.

In total, 13 specimens were used for Geometric morphometric analyses, including 6 specimens of *M. aistoodonnivalis*, 4 specimens of *M. nivalis* and 3 *M. altaica.* External measurements measured in field, including head body length (HBL, from snout to the anus), tail length (TL), ear length (EL), and hind foot length excluding the claws (HFL). External measurements of *M. erminea* were from Gao *et al*. (1987). For geometric morphometric analysis, we chose the complete adult individual skull to use in morphological analyses. Dorsal,

ventral and lateral views of the cranium, as well as lateral views of the mandible were photographed (Nikon D800 camera with a Nikon AF-S 105 mm f2.8G IF-ED microlens). In order to ensure that the location of the photos taken was fixed, all photos were taken by the same person. When taking pictures on all sides of the specimen, the reference points on different shooting surfaces were selected to keep the relative positions of all the objects and the camera consistent, so that each shooting face was consistent in both the horizontal and vertical directions (Zelditch 2004).

TPS files were produced by TPSUTIL V1.65 (Rohlf 2015). All morphological photographs, which were evaluated in a random order by one investigator, were scaled, identified, and digitally landmarked and semi-landmarked using TPSDIG V2.22 (Rohlf 2015). All the landmarked were in accordance with the relevant animal skull marking methods and combined with the actual healing characteristics of the skulls of the specimens (Cardini and O'Higgins 2004). Landmarks were homologs and they were identified consistently in all photographs. Semi-landmarks were useful for depicting the shape of curved lines where landmarks could not be detected (Zelditch *et al*. 2004; Sansalone *et al.* 2015). The location of the marked and semi-marked points was shown in Figure 2.

All configuration sets for our 13 specimens were superimposed using the generalized Procrustes analysis (GPA) in the program COORDGEN8 (Bookstein 1997). This least squares-based superimposition standardized the configuration sets for an overall position, scale and orientation, yielding a set of shape coordinates for each photograph. Next, principal component analyses (PCA) were employed and the ordination of the aligned specimens visualized in scatterplots using the program PCAGEN8 (Sheets 2014). The shape parameters of the specimen were converted into thin lath coefficients, that is, partial warps scores, and we calculated the covariance matrix of the local warps index (Sheets 2012). The PC axes corresponded to eigenvectors of the variance-covariance matrix for the shape data, and eigenvalues were assumed to be proportional to the variance explained by the PCS (Zelditch *et al*. 2004). The shape deformations along the first and second principal component axes were illustrated in grids and vectors. Transformed grids represented the actual differences in the location of landmarks (or semi-landmarks), and the length and direction of the black line on each landmark (or semi-landmark) represented the degree and orientation of the deformation, respectively.

According to the different clusters, the principal component analysis method was used to analyze all the specimens to discuss the differences with MORPHOLOGIKA 2.2.5 software.

Results.

Sequence information.

We obtained 24 new *cyt b* sequences [1140 bp], 15 *Rag1*[1064 bp], 15 *Rag2* [456 bp], 15 *ATP7A* [636 bp], 15 *BDNF* [536 bp], 15 *TMEM20* [596 bp] and 15 *Apob*[907 bp]. In addition, 18 *cyt b*, 15 *Rag1*, 15 *Rag2*, 15 *ATP7A*, 15 *BDNF,* 15 *TMEM20* and 15 *Apob* were downloaded from GenBank for phylogenetic analysis. All new sequences were deposited in GenBank.

Phylogenetic analysis.

Phylogenetic results are shown in the figure 3. In the phylogenetic tree, the *cyt b* gene tree recovered seventeen major monophyletic clades. The first basal clade in *Mustela* consisted of *Neovison vison, M. felipei, M. africana* and *M. frenata*none. *Neovison vison* is not native to China, and the two samples we collected may have been individuals that escaped from local farms. *M. aistoodonnivalis* did not cluster with *M. nivalis* but formed a monophyletic group with *M. erminea* that was not significantly supported (pp=0.45). *M. altaica* and *M. nivalis*

formed a monophyletic clade that was significantly supported (pp=1.00).

Phylogenetic trees obtained from nuclear genes were similar to those obtained from phylogenetic trees of *the cyt b* gene. These analyses strongly support the clustering of *M. aistoodonnivalis* and *M. erminea* into a monophyletic group (pp=1.00). At the same time, we also observed that *M. aistoodonnivalis* and *M. nivalis* were not on the same branch (Fig.3).

In the combined phylogenetic tree of mitochondrial and nuclear genes, *M. aistoodonnivalis* and *M. erminea* were still clustered together, but the support rate was low (Fig.3).

According to the genetic distance results (Table 4), the *cyt b* p-distances among the species of *Mustela* ranged from 0.009 to 0.150. The smallest p-distance occurred between *M. lutreola* and *M. putorius* (0.009), and the largest one occurred between *M. africana* and *M. nudipes* (0.150). The p-distances between *M. nivalis* and *M. aistoodonnivalis* was 0.091, between *M. erminea* and *M. aistoodonnivalis* was 0.075.

Table 4 Mean *cyt* b distance between candidate species calculated using the Kimura 2 parameter model

	1	2	3	4	5	6	7	8	9	10	11	12	13	14	15	16
1 *M. nivalis*																
2 *M. aistoodonnivalis*	0.091															
3 *M. altaica*	0.076	0.094														
4 *M. sibirica*	0.083	0.087	0.087													
5 *M. V*	0.134	0.127	0.127	0.122												
6 *M. africana*	0.133	0.125	0.126	0.126	0.112											
7 *M. erminea*	0.080	0.075	0.073	0.082	0.116	0.117										
8 *M. eversmanni*	0.081	0.081	0.086	0.041	0.122	0.126	0.081									
9 *M. felipei*	0.127	0.115	0.120	0.124	0.100	0.072	0.107	0.121								
10 *M. frenata*	0.126	0.116	0.126	0.120	0.103	0.070	0.112	0.119	0.068							
11 *M. itatsi*	0.082	0.082	0.099	0.051	0.120	0.128	0.078	0.053	0.111	0.114						
12 *M. kathiah*	0.119	0.111	0.126	0.118	0.137	0.131	0.109	0.122	0.130	0.126	0.114					
13 *M. lutreola*	0.081	0.084	0.085	0.038	0.123	0.126	0.081	0.010	0.119	0.117	0.052	0.124				
14 *M. nigripes*	0.083	0.086	0.090	0.043	0.128	0.128	0.084	0.026	0.123	0.117	0.055	0.123	0.026			
15 *M. nudipes*	0.143	0.129	0.140	0.136	0.136	0.150	0.123	0.142	0.136	0.144	0.135	0.136	0.139	0.141		
16 *M. putorius*	0.081	0.085	0.081	0.040	0.122	0.122	0.082	0.013	0.118	0.118	0.056	0.123	0.009	0.028	0.138	
17 *M. strigidorsa*	0.115	0.128	0.134	0.128	0.124	0.134	0.117	0.127	0.122	0.133	0.124	0.134	0.124	0.130	0.110	0.124

Species identification. ——According to GMYC analysis (Fig.4), the branch line formed earlier than 0.01 Ma was assumed to be a valid species, therefore, A-J 12 branches were considered to be valid species. Among them, *M. aistoodonnivalis* was determined to be a separate species, which was consistent with the conclusion drawn on the phylogenetic tree.

The topological structure of the *BEAST species-tree was similar to that of phylogenetic tree. *M. aistoodonnivalis* and *M. erminea* were moderately supported as two separate species (pp=0.85), and *M. nivalis* did not gather on the same branch with *M. aistoodonnivalis* (Fig.5).

BPP analysis obtained 12 groups of analysis results (Table 5), all of them significantly supported *M. aistoodonnivalis* as a single species (PP = 1.0). At the same time, the 12 sets of data also supported *M. aistoodonnivalis* and *M. nivalis* as independent species, with significant support (PP=1.0).

Table 5 Support rate of BPP species definition under different algorithms and prior parameters for *Mustela*

MDNA-algorithm0	**Species delimitation**	1 0 2	1 0 10	1 0 20	1 0 2	1 0 10	1 0 2=	Menn（pp）
		Heredity= 1 1 4	Heredity= 1 1 4	Heredity= 1 1 4	Locustrate = 1 1 10	Locustrate=1 1 10	Locustrate=1 1 10	
Mustela aistoodonnivalis, M. erminea		1	1	1	1	1	1	1
(*Mustela aistoodonnivalis, M. erminea*), *M. nivalis*		1	1	1	1	1	1	1
Inl（mean）		-11670.255726	-11670.433553	-11669.838123	-11694.008780	-11693.841117	-11693.624311	
SD[InL（medium）]		10.110621	10.075418	9.998659	9.626029	9.672850	9.612990	
MDNA-algorithm1	**Species delimitation**	1 1 1.5 1	1 1 1 0.5	1 1 2 2	1 1 1.5 1	1 1 1 1.5 1	1 1 2 2	Menn（pp）
		Heredity= 1 1 4	Heredity= 1 1 4	Heredity= 1 1 4	Locustrate = 1 1 10	Locustrate=1 1 10	Locustrate=1 1 10	
Mustela aistoodonnivalis, M. erminea		1	1	1	1	1	1	1
(*Mustela aistoodonnivalis, M. erminea*), *M. nivalis*		1	1	1	1	1	1	1
Inl（mean）		-11670.616828	-11670.085622	-11669.911678	-11693.962989	-11694.245867	-11694.136618	
SD[InL（medium）]		10.230402	10.257863	10.102949	9.684815	9.632297	9.660039	

Morphological analysis

Principal component analysis based on digitized results of three species of the front side showed that the first three principal component eigenvalues accounted for 59.63% of the overall variable. Plotting the first principal component and the second principal component, the markers mixed together and there were no major differences in the skulls of the 3 species of *Mustela* (Fig.6a).

Principal component analysis based on digitized results of the side of the *Mustela* skull showed that the first three principal component eigenvalues accounted for 84.49% of the overall variable. Plotting the first principal component and the second principal component, the markers also mixed together and there were no major differences in the skulls of the 3 species of *Mustela.* These results are consistent with the result of the front side of the skull (Fig.6b).

Principal component analysis based on digitized results of the backside of the skull showed that the first three principal component eigenvalues accounted for 75.61% of the overall variable. Plotting the first principal component and the second principal component, we found that there was a more obvious difference between *M. aistoodonnivalis* and the other two species of *Mustela*, and that the markers of *M. aistoodonnivalis* mainly concentrated in the negative region of the second principal component (Fig.6c).

Principal component analysis based on digitized results of mandible showed that the first three principal component eigenvalues accounted for 90.53% of the overall variable. Plotting the first principal component and the second principal component, we found that there was a more obvious difference between *M. aistoodonnivalis* and the other two species of *Mustela*, and that the markers of *M. aistoodonnivalis* mainly concentrated in the positive region of the second principal component (Fig.6d).

Morphological comparison among *M. aistoodonnivalis*, *M. nivalis* and *M. erminea* listed in Table 6 and showed in Figure 7-8. Figure 7 showed that the first incisor of *M. aistoodonnivalis* locates at anteromedial of second incisor; but in *M. nivalis* and *M. ermine,* three incisors arrange as a line; the most obvious distinguishing feature was that *M. aistoodonnivalis* lacked the second lower molar, while *M. nivalis* and *M. erminea* had the second molar. On appearance and pelage, dorsal hairs of *M. nivalis* were light brown-red, but in *M. aistoodonnivalis*, they were dark brown; the venter hairs of *M. nivalis* are white or pale, while in *M. aistoodonnivalis,* belly was light yellow with rusty red patches, throat and ventral of cheek are white. Thirdly, in *M. nivalis*, the back of the limbs was white, but in *M. aistoodonnivalis*, the back of the limbs were the same color as the back hair, which was dark brown, and claws and palms of half specimens cover with white hair. Pelage of *M. ermine* differs from *M. aistoodonnivalis* and *M. nivalis* in many aspects. Summer coat of *M. ermine* was gray-brown, belly was pure white; 1/3 terminal of tail is black; back of feet were gray-white (Table 6 and Fig. 8). For measurements, *M. erminea* was much larger than *M. aistoodonnivalis* and *M. nivalis.* TL/HBL of *M. aistoodonnivalis* > *M. nivalis* > *M. ermine* (Table. 6).

Table 6. Morphological comparison anomg *M. aistoodonnivalis*, *M. nivalis and M. ermine**

		M. aistoodonnivalis	*M. nivalis*	*M. erminea*
coat color	dorsum	dark brown (summer)	light brown-red (summer)	grayish brown (summer)
			white (winter)	white (winter)
	abdomen	light yellow	white or pale	white
	tail	dark brown around tail	light brown	Tip black
	forelimb	dark brown	white	white
appearance	HBL	150mm (127.8-165.2mm)	170 mm (157-183mm)	217mm (190-220mm)
	TL	70mm (50-62mm)	55 mm (20-53mm)	42 mm (42-80mm)
	TL/HBL	46.7%	32.4%	19.4%
skull	profile length	30.49mm (29.79-34.16mm)	33.47mm (32.12-35.17mm)	43.30mm (35.20-41.70mm)
	zygomatic breadth	15.65mm (14.83-16.53mm)	16.77mm (16.37-18.07mm)	23.50mm (19.30-24.10mm)
	M_2	missing	existing	existing
	dental formula	3.1.3.1/2.1.3.1=32	3.1.3.1/3.1.3.2=34	3.1.3.1/3.1.3.2=34

*Abbreviations see method.

Discussion.

Our analyses of *cytb,* six nuclear genes and *ctyb+* six nuclear genes resolved that *M. aistoodonnivalis* and *M. erminea* clustered togather with medium or lower support, and *M. aistoodonnivalis* never sistered with *M. nivalis.* The species delimitation analysis showed that *M. aistoodonnivalis* was valid species. The p-distances between *M. nivalis* and *M. aistoodonnivalis* was 0.091, between *M. erminea* and *M. aistoodonnivalis* was 0.075. PCA analysis based on mandible showed obvious difference between *M. aistoodonnivalis* with *M. nivalis* and *M. ermine.* Measurements and pelage among *M. aistoodonnivalis*, *M. nivalis* and *M. ermine* showed significant difference. In conclusion, on the basis of molecular and morphological analyses, we recognized *M. aistoodonnivalis* as valid species.

According to the latest classification, there were five subgenera and seven species of *Mustela* in China: *Mustela* (*M. erminea*), *Gale* (*M. nivalis*, *M. altaica* and *M. kathiah*), *Putorius* (*M. eversmannii*), *Kolonokus* (*M. sibirica*) and *Gryptomustela* (*M. strigidorsa*) (Abramov 2000). Phylogenetic analysis clustered *M. aistoodonnivalis* with *M. ermine.* P-distance between *M. aistoodonnivalis* and *M. erminea* was much larger than the average genetic distance between subgenera. But relationship of *M. aistoodonnivalis* was uncertain because of lower support of lineage, the subgenus status

of *M. aistoodonnivalis* needed further studied.

Ackonwledgment.

This research was founded by the National Natural Science Foundation of China (31970399, 31670388). We are grateful to Zhao Lianjun for assistant for collecting specimens.

References.

Allen G M (1938) The mammals of China and Mongolia (Natural History of Central Asia). W. Granger, editor. Central Asiatic Expeditions of the American Museum of Natural History 11:1-620.

Abramov A V (2000) A taxonomic review of genus Mustela (Mammalia, Carnivora) Zoosystematica Rossica 8:357-364.

Bradley R D, Baker R J (2001) A test of the genetic species concept: Cytochrome-b sequences and mammals. Journal of Mammalogy 82(4), 960-973.

Bookstein F L (1997) Morphometric tools for landmark data: geometry and biology. Cambridge University Press.

Cardini A, O'higgins P (2004) Patterns of morphological evolution in Marmota (Rodentia, Sciuridae): geometric morphometrics of the cranium in the context of marmot phylogeny, ecology and conservation. Biological Journal of the Linnean Society 82(3): 385-407.

Corbet G B, Hill J E (1992) Mammals of the Indomalayon Region. A Systematic Review. Oxford University Press: Oxford.

Darriba D, Taboada G L, Doallo R, Posada D (2012) JModelTest 2: More models, new heuristics and parallel computing. Nat Methods 9, 772.

Drummond A J, Suchard M A, Xie D, Rambaut A (2012) Bayesian phylogenetics with BEAUti and the BEAST 1.7. Molecular Biology & Evolution 29(8), 1969-1973.

Ellerman J R, T C S Morrison-Scott (1951). Checklist of Palaearctic and Indian Mammals 1758 to 1946.Trustees of the British Museum (Natural History): London.

Fujisawa T, Barraclough T G (2013) Delimiting Species Using Single-Locus Data and the Generalized Mixed Yule Coalescent Approach: A Revised Method and Evaluation on Simulated Data Sets. Systematic Biology 62(5), 707-724.

Gao Y T *et al.* (1987) Fauna Sinica: Mammalia Volume 8: Carnivora. Science Press.

Gong H S, Z G Zeng, X B Gao (2009) Discussion on the Changes of the List of Key Species of Wildlife within Provincial-protection in Shaanxi 2009.24(1).107-115.

Heather A, Klaus-Peter K (2003) A new phylogenetic marker, apolipoprotein B, provides compelling evidence for eutherian relationships. Molecular Phylogenetics and Evolution, 28(2).

Hutterer, R (2005) Order Soricomorpha. In: D. E. Wilson & D. A. Reeder, e. (Ed.), Mammal Species of the World: A taxonomic and geographic reference. John Hopkins University Press, Baltimore, pp. 220–311.

Heled J, Drummond A J (2010) Bayesian Inference of Species Trees from Multilocus Data. Molecular Biology & Evolution 27(3), 570-580.

Heptner V G (1967) Mlekopitayushchie Sovetskovo Soyuza. Morskie kotovy i khishehnye [Mammals of the Soviet Union. Sea cows and Carnivores.] (V. G. Heptner and N. P. Naumov, eds.). Vysshaya Shkola 2(1):1-1004 (in Russian).

Hu J Z, J Hu (2007) Newly Edited Catalogue of Sichuan Mammals[J]. Journal of China West Normal University (Natural Sciences) 28(3):165-171.

Huelsenbeck J P, Rannala B (2004)Frequentist Properties of Bayesian Posterior Probabilities of Phylogenetic Trees under Simple and Complex Substitution Models. Systematic Biology 53(6), 904-913.

Irwin D M, Kocher T D, Wilson A C (1991Evolution of the cytochrome b gene of mammals.

Journal of molecular evolution 32(2).
Jiang Z. G., Y. Ma, Y. Wu, Y. X. Wang, K. Y. Zhou, Z. J. Feng, S. Y. Liu, Z. H. Luo, C. W. Li. (2015). China's mammalian diversity. Biodiversity Science 23 (3): 351–364
Jiang Z G, S Y Liu, X L Jiang, K Y Zhou (2017) China's mammalian diversity. Biodiversity Science 25(08):886-895.
Lin L K, Motokawa M (2010) A New Subspecies of the Least Weasel *Mustela nivalis* (Mammalia, Carnivora) from Taiwan. Mammal Study 35(Sep 2010):191-200.
Lindblad-Toh K, Wade C M, Mikkelsen T S, Karlsson E K, Jaffe D B, Kamal M, *et al.*(2005) Genome sequence, comparative analysis and haplotype structure of the domestic dog. Nature 438, 803-819.
Linnaeus C (1766-1768) Systema naturae per regna tria naturae, secundum classes, ordines, genera, species, cum characteribus, differentiis synonymis, locis. Vol. 1. Regnum Animale. pt. 1, pp. 1- 532 [1766]; vol. 3, Appendix pp. 223-235 [1768]. 12th ed. [Vol. 3, Regnum Lapideum, pp. 1- 222,
Mittermeier R A, Wilson D E (2009) Handbook of the Mammals of the World – Volume 1: Carnivores, Sloths and Colugos. Barcelona: Lynx Edicions.
Murphy W J, Eizirik E, Johnson W E, Zhang Y P, Ryder O A, O'Brien S J (2001) Molecular phylogenetics and the origins of placental mammals. Nature 409(6820).
Nei M, Kumar S (2000) Molecular evolution and phylogenetics[M]. Molecular evolution and phylogenetics. Oxford University Press.
Paradis E, Claude J, Strimmer K (2004) APE: Analyses of Phylogenetics and Evolution in R language. Bioinformatics 20(2), 289-290.
Pons J, Barraclough T G, Gomez-Zurita J, Cardoso A, Duran D P, Hazell S, (2006) Sequence-Based Species Delimitation for the DNA Taxonomy of Undescribed Insects. Systematic Biology 55(4), 595-609.
Rohlf F J (2015) The tps series of software. Hystrix, the Italian Journal of Mammalogy, 26, 9–12.https://doi.org/10.4404/hystrix-26.1-11264.
Ruan S J, H S Gong (1999) Mammmals resources in Niubeiliang national natural reserve,shaanxi province[J]. Chinese Journal of Zoology 34(2):30-35.
Sambrook J, Fritsch E F, Maniatis T (1989) Molecular cloning: a laboratory manual. Cold Spring Harbor Laboratories.
Sansalone G, Kotsakis T, Piras P (2015) Talpa fossilis or Talpa europaea? using geometric morphometrics and allometric trajectories of humeral moles remains from Hungary to answer a taxonomic debate. Palaeontologia Electronica 18, 1-17. Https://doi.org/10.26978.
Smith A T, Y Xie (2009) A guide to the mammals of China. Hunan Education Publishing House, Changsha (In Chinese).
Qing Y, Y B Zhou, D W Qi, W G Zhang, X Q Wang, C Li, J Z Hu (2004)Preliminary Investigation of Mammals in Xiaohegou Nature Reserve, Sichuan. Sichuan Journal of Zoology 23(2):142-145.
Pan Q H, Y X Wang, K Yan (2007) A field guide of the mammals of China[M]. China Forestry Publishing House.
Tamura K, Peterson D, Peterson N, Stecher G, Nei M, Kumar S (2011) MEGA5: Molecular Evolutionary Genetics Analysis Using Maximum Likelihood, Evolutionary Distance, and Maximum Parsimony Methods. Molecular Biology & Evolution 28(10), 2731.
Teeling E C, Scally M, Kao D J, LRomagnoli M, Springer M S, Stanhope M J (2000) Molecular evidence regarding the origin of echolocation and flight in bats. Nature 403(6766).
Thomas O (1911a) The mammals of the tenth edition of Linnaeus; an attempt to fix the types of the genera and the exact bases and localities of the species. Proceedings of the Zoological Society of London, 1911:120-158.
Wang Y X (2003) A complete checklist of mammal species and subspecies in China[M]. China

Forestry Publishing House.
Wu J Y, and Y T Kao (1991) A new species of mammals in China—Lackedteeth pygmy weasel (*Mustela aistoodonnivalis* sp,nov.). Journal of Northwest University (Natural Science Edition) 1991 supplement,87-93.
Yang Z, Rannala B. (2010) Bayesian species delimitation using multilocus sequence data[J]. Proceedings of the National Academy of Sciences 107(20): 9264-9269.
Zelditch M L, Swiderski D L, Sheets H D, *et al*. (2004) Superimposition methods-Geometric Morphometrics for Biologists5. Geometric Morphometrics for Biologists 105–128.
Ziheng Y, Bruce R (2010) Bayesian species delimitation using multilocus sequence data. Proceedings of the National Academy of Sciences of the United States of America 107(20), 9264-9269.

Fig.1 Map of *Musteal*, showing localities sampled for this study.
Fig.2 The Schematic of marked and semi-marked points.
Fig.3 Bayesian phylogenetic analyses based on dataset 1(*cyt b*), dataset 2(combined genes of all six nuclear genes fragments) and dataset 3(combined genes of all six nuclear genes and *cyt b* fragments). Node number indicat.
Fig.4 Results of species delimitation using splits in R for *Mustela*.
Fig.5 Results of species delimitation mtDNA+nDNA gene species trees using the BEAST model. Node numbers indicate Bayesian posterior probabilities supporting.
Fig.6 Principal component analysis and deformation vector of skull.
Fig.7 The comparison of the back side and the mandible among *Mustela aistoodonnivalis*, *Mustela nivalis*.and *Mustela erminea*.
Fig.8 The specimen comparison between *Mustela aistoodonnivalis* and *Mustela nivalis*.

ARPHA Preprints *Author-formatted, not peer-reviewed document posted on 27/07/2021.* DOI: https://doi.org/10.3897/arphapreprints.e72208

Figure 1 Map of *Mustela*, showing localities sampled for this study.

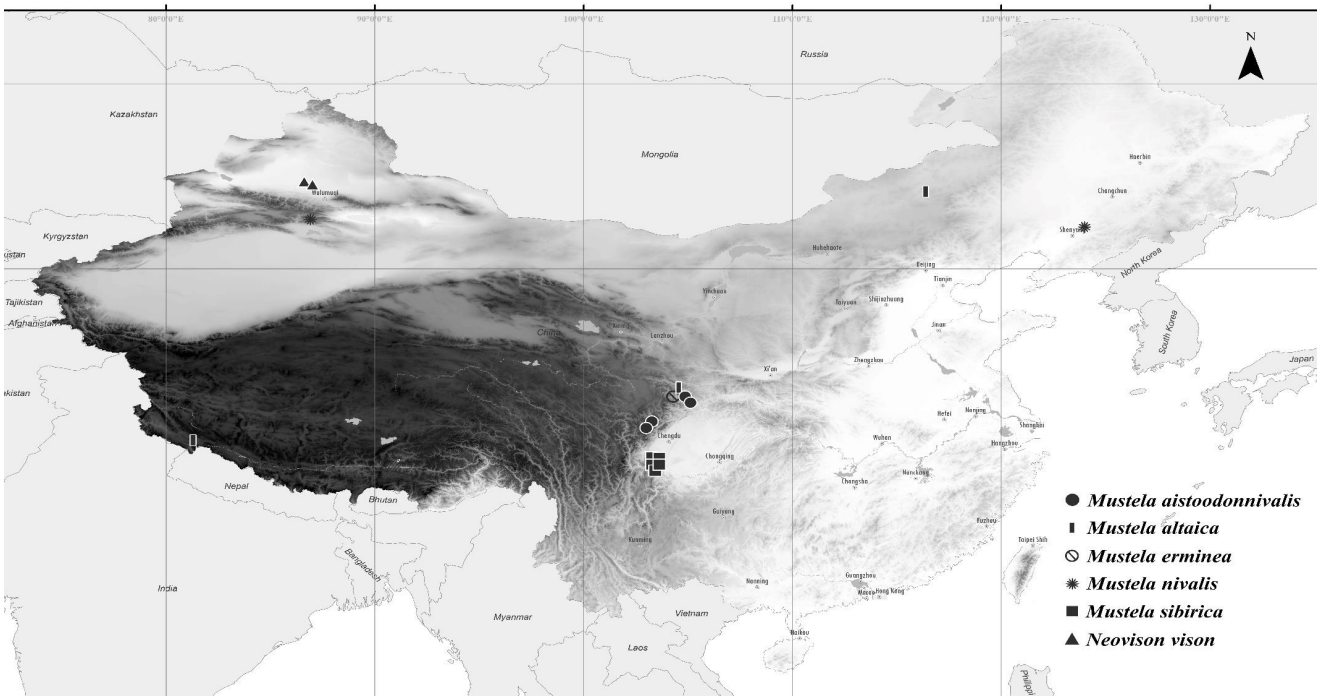

Figure 2 The Schematic of marked and semi-marked points

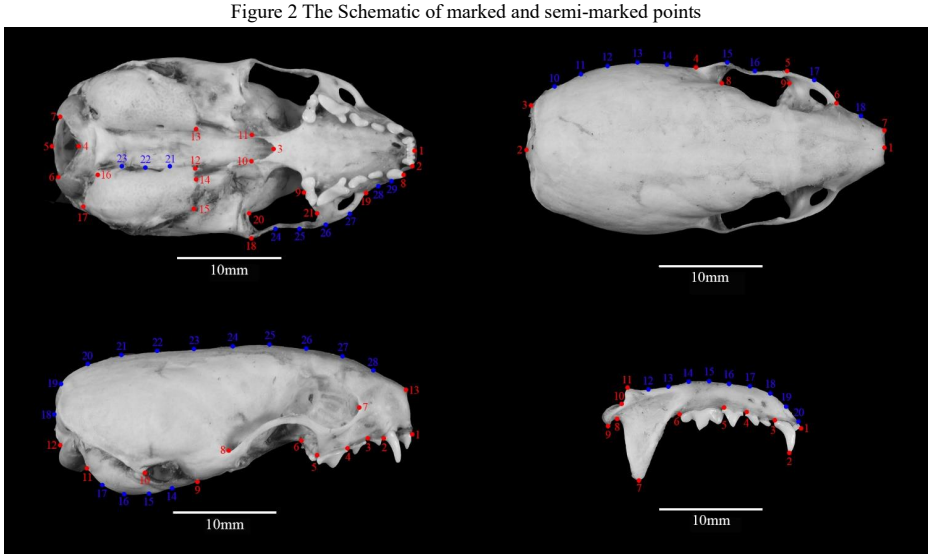

Figure 3 Bayesian phylogenetic analyses based on dataset 1(*cyt b*), dataset 2(combined genes of all six nuclear genes fragments) and dataset 3(combined genes of all six nuclear genes and *cyt b* fragments). Node number indicat

Figure 4 Results of species delimitation using splits in R for *Mustela*

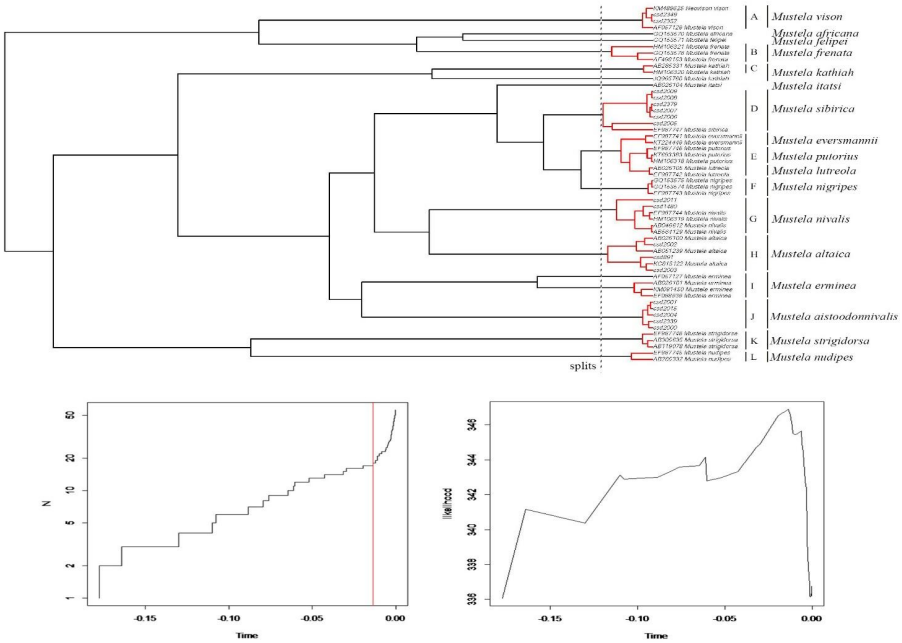

Figure 5 Results of species delimitation mtDNA+nDNA gene species trees using the BEAST model. Node numbers indicate Bayesian posterior probabilities supporting

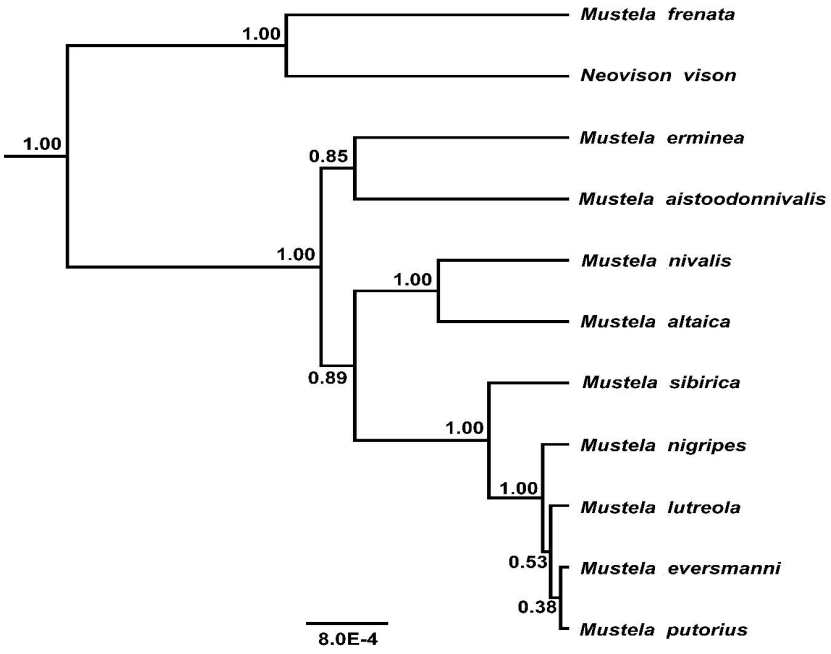

ARPHA Preprints *Author-formatted, not peer-reviewed document posted on 27/07/2021.* DOI: https://doi.org/10.3897/arphapreprints.e72208

Figure 6 Principal component analysis and deformation vector of skull

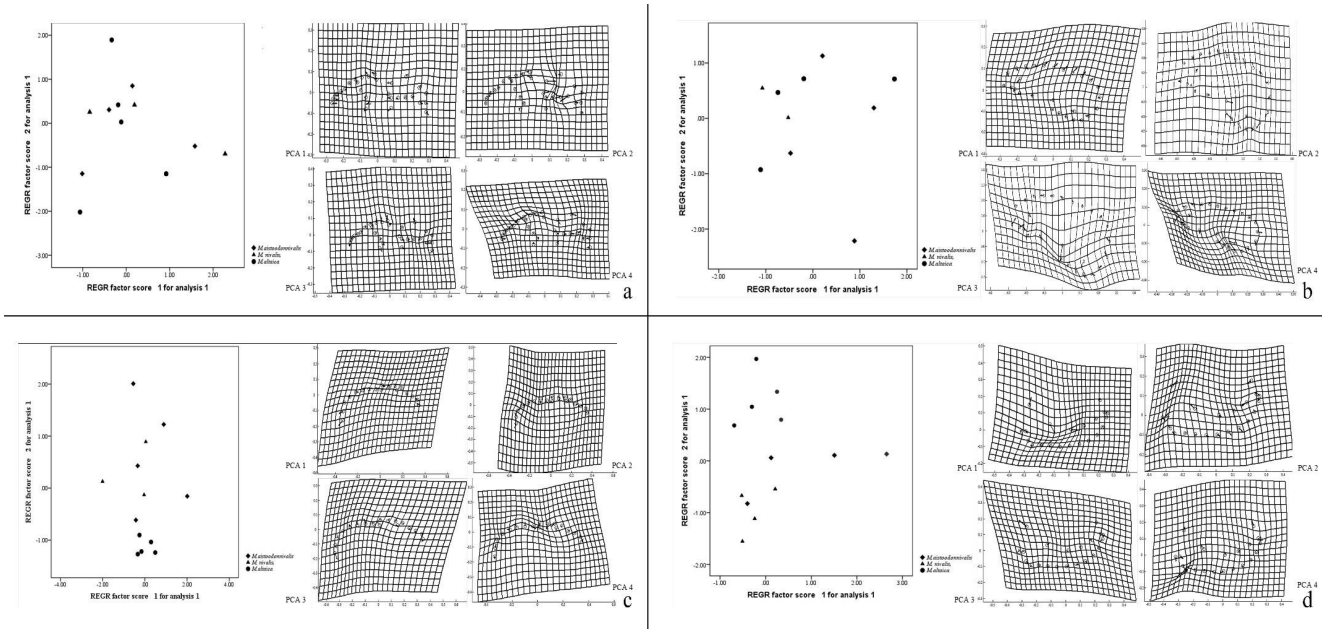

ARPHA Preprints *Author-formatted, not peer-reviewed document posted on 27/07/2021.* DOI: https://doi.org/10.3897/arphapreprints.e72208

Figure 7 The comparison of the back side and the mandible among *Mustela aistoodonnivalis*, *Mustela nivalis*.and *Mustela erminea.*

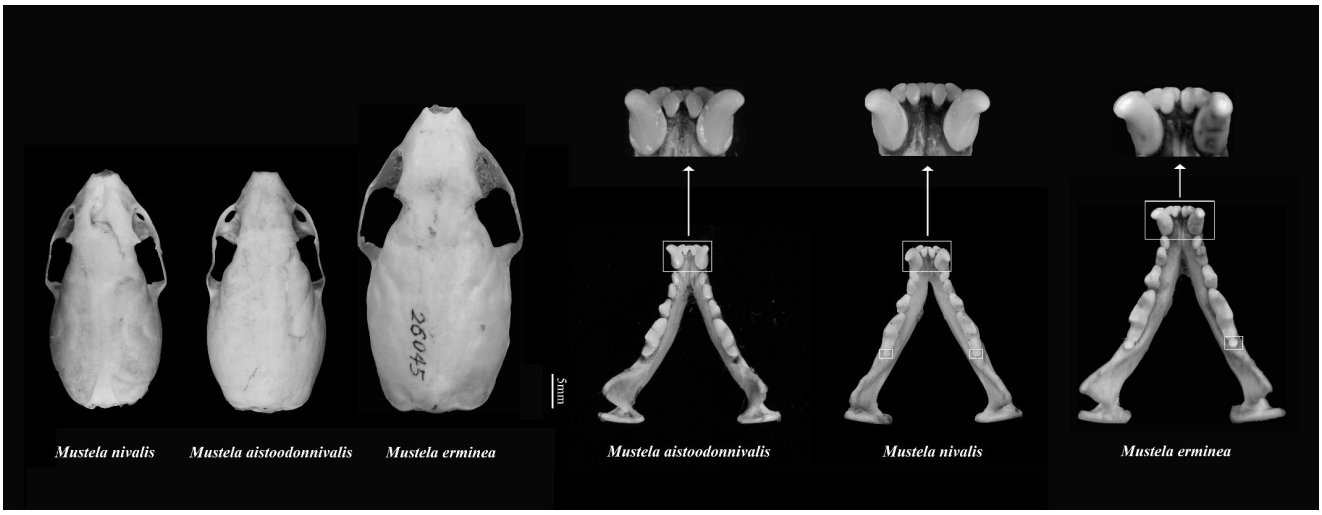

Figure 8 the specimen comparison between *Mustela aistoodonnivalis* and *Mustela nivalis*